Uncertainty Analysis of Large-scale Power Systems Using Collocation

Josh A. Taylor, Franz S. Hover
Massachusetts Institute of Technology
Department of Mechanical Engineering
jatl@mit.edu, hover@mit.edu

Abdelhamid Ouroua
University of Texas at Austin
Center for Electromechanics
a.ouroua@mail.utexas.edu

Keywords: Collocation, uncertainty, sparse grid, dimension-adaptive, pulse power system

Abstract

Collocation algorithms for efficiently solving stochastic differential equations arising from modeling uncertainty in large-scale systems are presented. The resulting solutions are integrated to compute statistical moments, from which sensitivity can be inferred, and interpolated to propagate PDF's. We give a detailed exposition of this approach, focusing on the dimension-adaptive algorithm of [10]. We give applications on a double pendulum, an integrated shipboard power system, and a pulse power system.

1. INTRODUCTION

Large-scale engineered systems pose a class of design problems for which there is currently no existing comprehensive approach. Dimensionality renders the space of possible realizations for such systems immense, placing them well outside the computational limits of traditional techniques. The all-electric ship is a representative example of large-scale systems, and its development is of significant interest to the control and simulation communities [6, 16]. Its superiority over current ships includes high efficiency power transfer through the ship, rapid reconfiguration, layout flexibility, and azimuthing thrusters providing enhanced maneuvering and hydrodynamic efficiency; presently, this is only a potential. To find designs and corresponding control strategies that attain this potential, the system must be considered as a whole; this requirement makes the electric ship a large-scale system.

In addition to large design spaces, numerous environmental interactions and inaccurate system information make uncertainty a necessary consideration. Solving the resulting stochastic differential equations is essentially a problem of representing the system as a function over a random space. Collocation algorithms accomplish this by sampling the system over its random space at special points, where in the case of large-scale systems a 'sample' is a simulation or experiment with uncertain parameters set according to the location of the sample. Simulation of and experimentation with large-scale systems is expensive, so we seek an accurate representation of the system from a minimal number of samples. There are multiple approaches, including brute force Monte Carlo, polynomial chaos [25], and collocation, the latter of which we focus on here[1].

2. BACKGROUND

2.1. Stochastic Differential Equations

Uncertainty can be incorporated into dynamical systems by modeling them with stochastic differential equations [15, 18]. From a general perspective, we seek the solution $u : \Omega \times \Re^+ \rightarrow \Re$ to

$$L(t,\omega;u) = f(t,\omega), \quad u_0 = g(\omega), \quad t \in \Re^+, \quad \omega \in \Omega, \quad (1)$$

where L is the differential operator and Ω the random space [26]. Statistical moments, such as means and variances, and PDF's are the typical information gained from solutions to (1). Equation (1) may contain both random variables and processes. A random process may be represented by a random variable at each moment in time; this however makes the sample space Ω infinite dimensional, a feature that cannot be directly accommodated computationally. The Karhunen-Loeve expansion [11] offers a means to approximate random processes using a finite number of random variables in a truncated spectral expansion. However, this can be unwieldy, as accurately representing a random process tends to dramatically increase the dimension of Ω.

2.2. Collocation

Collocation approximates solutions to (1) by calculating solutions of deterministic differential equations corresponding to special points in the random space Ω and then using those solutions to construct a function over Ω at each moment in time. Monte Carlo methods differ only in the choice of points, using pseudo- or quasi-random points rather than collocation points. At this point, it is sensible to simplify the discussion from stochastic differential equations to functions; a solution to a stochastic differential equation at a fixed time is essentially a function over a random space, and in the case of collocation, finding that solution amounts to approximating a function at each instant in time. Two basic settings in which collocation algorithms are used are numerical integration and interpolation of functions.

[1] A Matlab implementation of the collocation algorithms in this paper is available at http://web.mit.edu/hovergroup/docs.html.

2.2.1. Numerical Integration

Numerical integration [3] is essentially a problem of efficiently characterizing a function over a space by sampling it at discrete points. All collocation algorithms considered here have implementations in numerical integration which can be expressed at as a sum of weighted function evaluations, such that the integral of a function f is approximated by

$$\int f(\mathbf{x})d\mathbf{x} \approx \sum_i w_i f(\mathbf{x}_i). \tag{2}$$

where the x_i are points at which f is evaluated and the w_i corresponding weights. A key product of solving stochastic differential equations is obtained through numerical integration: the statistical moments of solutions. In addition to knowing mean behaviors, variance trajectories are indicative of a system's sensitivity to uncertainty as a function of time. We utilize integral and maximum definitions of sensitivity:

$$\text{Integral Sensitivity} = \int var(x(t))dt, \tag{3}$$

$$\text{Maximum Sensitivity} = \max_t\{var(x(t))\}. \tag{4}$$

Later, we make use of these quantities in our analyses in the applications section.

2.2.2. Interpolation

Interpolation [1, 4, 14] is very like numerical integration, except that we are now evaluating rather than integrating a function approximation. In the context of interpolation, function approximations are often referred to as interpolants.

The one-dimensional barycentric interpolation formula of the second form is preferable for its numerical stability and computationally efficiency. It is given by

$$P_q[f](x) = \frac{\sum_i \frac{l_i}{x-x_i} f(x_i)}{\sum_i \frac{l_i}{x-x_i}}, \quad l_i = \prod_{j\neq i} \frac{1}{x_i - x_j}. \tag{5}$$

Interpolation can be used to approximate PDF's via histograms. A direct way to accomplish this without interpolation is with Monte Carlo: evaluate a function or simulate a system at random points and sort the outcomes into bins. However, direct evaluation can be costly; instead apply Monte Carlo to the interpolant, which is always cheap to evaluate, and generate histograms of interpolated function values or system simulations. Consider the Pulse Power Simulink model, which is studied in section 3.3.; one evaluation takes ten minutes, so directly applying Monte Carlo to create a 1,000 point histogram would be time consuming. Suppose the response can be characterized with fair accuracy using 100 collocation points. The simulation can now be interpolated 1,000 times to produce nearly the same histogram (the accuracy increases with the number of collocation points used) in the time it takes to simulate the system 100 times.

2.2.3. One-dimensional Function Approximation

A system often has multiple sources of uncertainty, yielding a multi-dimensional random space. With the exception of Monte Carlo, multi-dimensional algorithms are generally comprised of one-dimensional techniques extended to multiple dimensions via tensor, or, in the case of a hypercube, Cartesian products. In one-dimensional numerical integration, the set of evaluation points and weights is often referred to as a quadrature. Well known one-dimensional quadratures include Simpson's rule and Newton-Cotes formulas. Polynomial based approaches, which evaluate functions at roots of polynomials, often have more attractive rates of convergence, particularly when the solution $u(\Omega,t)$ is a smooth function of Ω. Polynomial based methods are measured by the order polynomial they will approximate exactly using a fixed number of points; this is known as polynomial exactness. Gaussian quadrature uses orthogonal polynomials, and has a high polynomial exactness of $2n-1$ [3, 12, 21]. Clenshaw-Curtis quadrature, which uses Chebyshev polynomials, achieves only n exactness, but is nested, an advantageous feature when using sparse grid or dimension-adaptive collocation [2, 24]. Gauss-Kronrod-Patterson quadrature, another nested sequence, begins with Gaussian quadrature and inserts Kronrod extension points to form a nested sequence of quadratures that has a polynomial exactness of $2n-1+m$, where n is the number of Gaussian quadrature points and m the number of extension points [7, 19].

2.2.4. Multi-dimensional Algorithms

As stated, multi-dimensional collocation algorithms are constructed by taking tensor products of one dimensional quadratures. The most basic technique is the full grid: it is a straightforward Cartesian product of each dimension's one dimensional basis quadrature Φ_q, and can be written

$$F_q^d = \Phi_q \otimes \cdots \otimes \Phi_q. \tag{6}$$

For numerical integration, it can be expressed as a weighted sum of function evaluations at each collocation point:

$$F_q^d[f] = \sum_{i_1=1}^{m_q} \cdots \sum_{i_d=1}^{m_q} w_{i_1} \cdot \ldots \cdot w_{i_d} f(x_{i_1}, \ldots, x_{i_d}), \tag{7}$$

where m_q is the number of points in the one-dimensional basis quadrature Φ_q. The full grid formulation is written here as having identical component quadratures in each dimension for notational concision, but this is not a requirement; any level of any valid rule may be used. This is often advantageous to keep in mind; a function that is poorly behaved in some dimensions and relatively smooth in others can be more efficiently approximated by using high resolution approximations in troublesome dimensions and lower resolution approximations in the others, rather than by using the same high resolution quadrature in every dimension.

With some information about the function being integrated, the integration error for full grid collocation with polynomial based component quadratures can be bounded. For functions in C^r (functions with bounded mixed derivatives up to order r), the error of full grid collocation is estimated by

$$|I[f] - F[f]| = O(n^{-r/d}) \tag{8}$$

where $I[f]$ is the exact integral and n the total number of function evaluations. The dimension factor d in the exponent is a manifestation of what is known as 'The Curse of Dimensionality'. As dimension grows, error order grows as well at an exponential rate. For low dimensional, smooth integrands, a full grid is often the best choice among non-adaptive methods.

In 1963, Smolyak introduced what is now known as Smolyak's formula and is the underlying formulation of all sparse grid methods [9, 14, 23]. Rather than using one high order tensor product, the sparse grid is a sum of lower order products, and tends to perform better in slightly higher dimensions than full grid approaches. Define the level i difference quadrature

$$\Delta_i = \Phi_i - \Phi_{i-1}, \quad \Delta_1 = \Phi_1.$$

Smolyak's formula can then be written

$$S_q^d = \sum_{|i|_1 < q+d} \Delta_{i_1} \otimes \cdots \otimes \Delta_{i_d}, \tag{9}$$

where $|i|_1 = i_1 + \cdots + i_d$.

At this point it becomes clear why nested component quadratures are preferable for sparse grids. Nesting causes points of different grids in the sum to coincide, and the number of common points increases with both the level and dimension of the sparse grid.

The error for a sparse grid with polynomial based component quadratures can be estimated in the same fashion as the full grid case:

$$|I[f] - S[f]| = O(n^{-r} log(n)^{(d-1)(r+1)}). \tag{10}$$

As with full grid collocation, the factor d eventually causes sparse grids to fall to 'The Curse' as well, but not as severely. The penalty incurred by dimension is mitigated by the $log(n)$ term, and consequently sparse grid collocation is often superior in mid-dimensional situations. Fig. 1 shows the evaluation points for a full and sparse grid.

Reference [10] presents a dimension-adaptive algorithm which places points according to online estimation of its convergence. Grids are chosen which have high resolution in dimensions over which the function is difficult to approximate, and low resolution in easier dimensions. Dimensional coupling is reacted to as well through high resolution joint grids. The basic building block of the dimension-adaptive algorithm

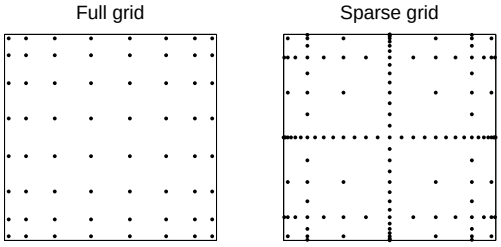

Figure 1. Left: Full grid with Legendre polynomial Gaussian quadrature. Right: Sparse grid with Gauss-Kronrod-Patterson quadrature.

is the difference quadrature Δ defined above. Fig. 2 illustrates the behavior of the algorithm on the function

$$f(\mathbf{x}) = \exp(-\sum_{i=1}^{2} |x_i - 0.5|). \tag{11}$$

This function is a two dimensional instantiation of one of six standard test functions from [8] widely used to evaluate the performance of numerical integration schemes.

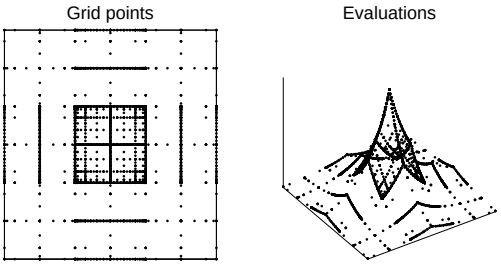

Figure 2. Nine element Clenshaw-Curtis dimension-adaptive integration of the two dimensional instantiation of a test function from [8]. The grid chosen by the algorithm are shown on the left, and the function evaluations at those points on the right.

To demonstrate the versatility of the algorithm, the space has been divided into nine identical elements, inside each of which the dimension-adaptive algorithm was executed. Multi-elements [13] is another powerful approach to solving stochastic differential equations, but which is not explored here. The function is C^0 along the central axes of the space, and analytic elsewhere. Grids that are of high order in the dimension perpendicular to the C^0 ridges are evaluated, while relatively low order grids are computed where the function is better behaved.

2.3. Appropriateness of Each Method

Full grids perform well in low dimensions and sparse grids in mid dimensions. In many situations, the dimension-

adaptive algorithm is superior to both, or at the least performs as well as the worst of the non-adaptive collocation schemes. Nested basis quadratures are desirable for sparse and dimension-adaptive grids despite their slightly lower polynomial exactness, because they permit reuse of function evaluations or system simulations.

It should be noted that due to 'The Curse of Dimensionality', Cartesian product based methods will invariably become ineffective in high enough dimension for all but trivial functions. Although it is not the focus of this paper, it is worth discussing the high-dimensional alternative: Monte Carlo. Pure Monte Carlo, or pseudo-randomness, converges according to the central limit theorem at $1/\sqrt{n}$, independently of dimension. Monte Carlo methods also do not depend on the smoothness of the integrand, and for badly behaved functions are sometimes superior even in low dimensions. Quasi-Monte Carlo [17] methods offer improvement to $1/n$ optimally and $\log(n)^d/n$ in the worst case. None of these are attractive rates, but in high dimensions they are often the best there is.

3. APPLICATIONS

We now demonstrate the use of these algorithms on three example systems: for illustrative purposes, a double pendulum, the Office of Naval Research Integrated Power System Testbed Simulink model (from Purdue), and a pulse power system Simulink model (from University of Texas at Austin).

3.1. Double Pendulum

Consider a freely falling double pendulum [22] with $\pm 1\%$ uniform uncertainty in the initial position and mass of each arm (Fig. 3). Initial conditions were $[\theta_1, \theta_2, \dot{\theta}_1, \dot{\theta}_2] = [\pi/2, \pi/2, 0, 0]$. Note that because there are four uncertain parameters, the system's random space is four-dimensional.

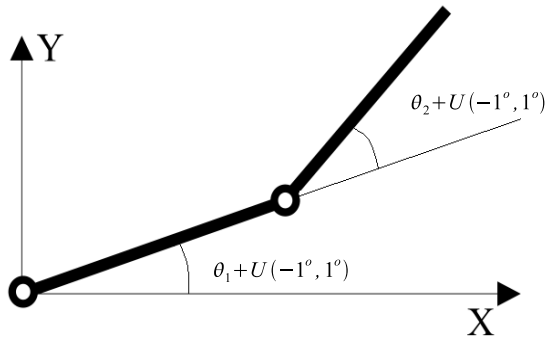

Figure 3. Double pendulum with uniform uncertainty in the initial positions and masses.

Dimension-adaptive collocation was used to compute a solution to the resulting system of stochastic differential equations. Deterministic solutions to the system equations at collocation points, i.e. realizations of the system, were generated using the fourth order Runge-Kutta scheme. 177 realizations were necessary for the adaptive algorithm to attain an error tolerance of 10^{-3}.

Fig. 4 shows mean trajectories with standard deviation envelopes for this system. Notice that at about 2.3 seconds the standard deviation grows very large. This is because the system after that time is sensitive to the prescribed uncertainty, meaning that it can exhibit a wide range of behavior depending on where in the random space the system is realized.

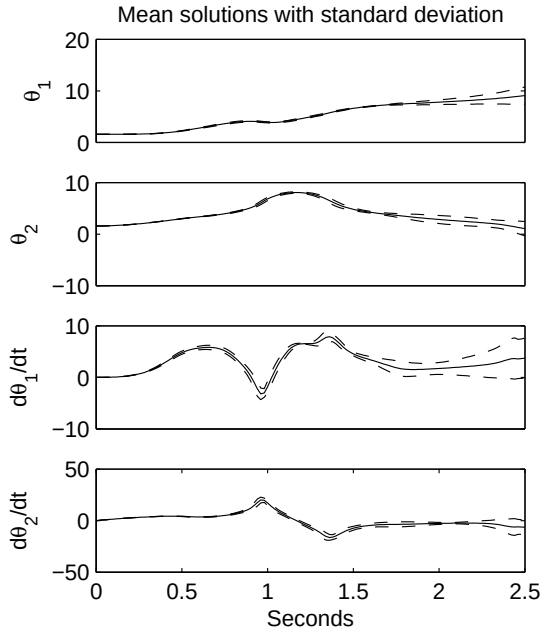

Figure 4. Mean solution with standard deviation envelope for a double pendulum with uniform initial position and mass uncertainty.

Fig. 5 shows 5,000 point histograms of each state at 2.5 seconds. Each used identical Monte Carlo points, that on the left generated by interpolation and on the right by direct simulation. The histograms agree fairly well. All have multiple modes, meaning that each arm can have substantially different positions and velocities depending on where in the random space the system is realized, and the interpolated histograms have captured this; this capability is critical for approaching real applications with confidence.

3.2. Integrated Power System Testbed

The Office of Naval Research Integrated Power System testbed Simulink model from Purdue (ONR IPS) [16, 20] (Fig. 6) describes the operation of a notional power system for the next generation all-electric ship. We examine uncertainty in the system by analyzing the statistical moments of

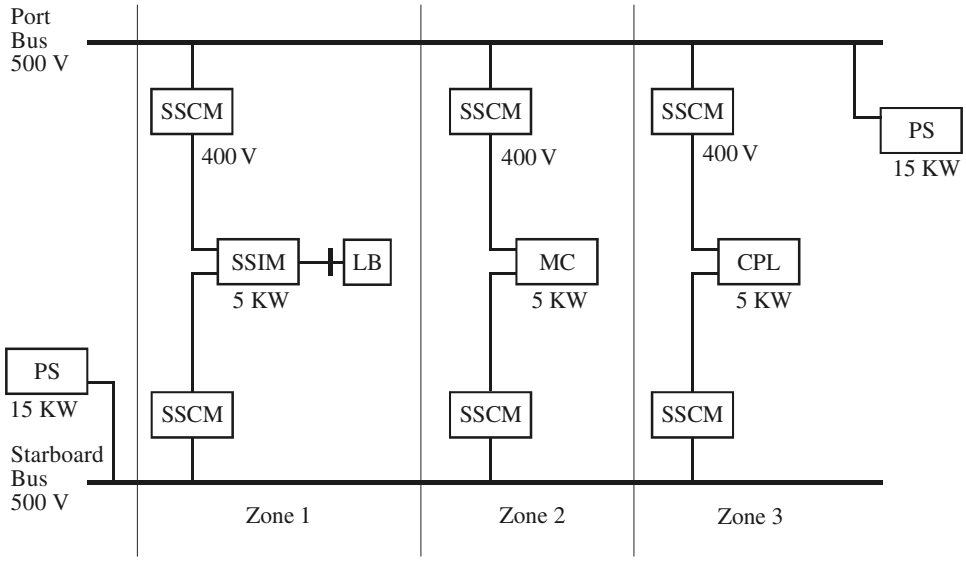

Figure 6. Schematic for ONR IPS Testbed.

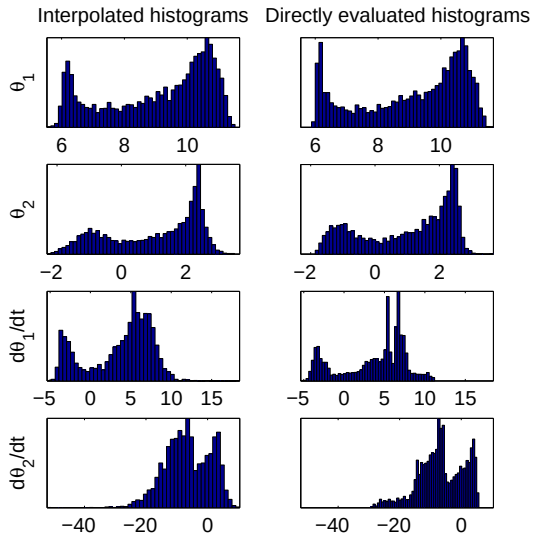

Figure 5. Interpolated and direct Monte Carlo histograms of double pendulum states at 2.5 seconds.

its responses. We vary parameters from the port and starboard AC systems, which contains the starboard generator, bus, and propulsion. In zone three, a constant power load, a proportional-integral controller, and two ship service converter modules are turned on, all at 0 seconds. At time 0.1 seconds, the motor and motor control turn on. At 0.4 seconds, the system is loaded from the ship service inverter module in zone one.

We give results from a three dimensional, level four full grid collocation simulation varying each uncertain parameter uniformly $\pm 1\%$ from its nominal value. We considered all possible triples (220 total runs) drawn from the set:

- Bus
  1, 7) C - Shunt Capacitance
  2, 8) C_f - Filter Capacitance
  3, 9) L_f - Filter Inductance

- Propulsion
  4, 10) C - Filter Capacitance
  5, 11) L - Filter Inductance
  6, 12) Induction Motor Mechanical Load

where parameters 1-6 are starboard and 7-12 port.

There are many ways to structure results from this sort of simulation, for example the most sensitive triple for a specific output: we find that triple $\{1,2,3\}$ is in fact the most influential triple for the starboard generator currents according to the integrated variance metric, and $\{1,2,5\}$ by the maximum metric. We present results that that are amenable to graphical analysis, but they are not the only perspectives.

Taking the most influential triple according to the integral metric, we compare the sensitivity of different output states. Since we are now comparing distinct outputs with different

units, we normalize the integrated variance by the integral of the square of the deterministic solution at the center of the random space. The output states corresponding to each number are listed below.

- Zone 3 DC states
  1) Load Voltage
  2) Starboard Voltage
  3) Starboard Current
  4) Port Voltage
  5) Port Current

- Starboard AC system states
  6-8) Voltages a,b,c
  9-11) Generator Currents a,b,c
  12-14) Propulsion Currents a,b,c
  15-17) Power Supply Currents a,b,c

The top plot in Fig. 7 shows the normalized integrated variances (NIV) of the output states, from which it is seen that the three most sensitive outputs to the triple $\{1,2,3\}$ are the power supply currents. The lower plot is of the multi-dimensional integral sensitivity (MIS), which we define as the square root of the normalized variance divided by the sum of the variance of the uncertain parameters in the simulation. This reflects the ratio of the standard deviation of the measured states to the standard deviation of the uncertain inputs. It appears that there is an eightfold increase in the variation of

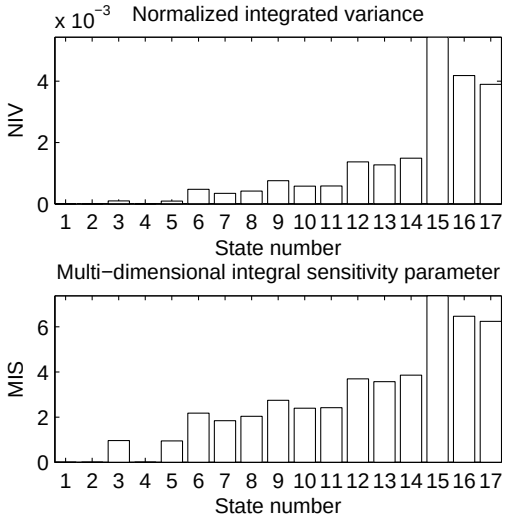

Figure 7. Starboard AC system normalized integrated variances (NIV) and multi-dimensional integral sensitivity (MIS).

the power supply currents, which is not very reassuring. But this is only for $\pm 1\%$ uncertainty. Fig. 8 shows the integrated variances (above) and multi-dimensional sensitivities (below) of the power supply currents for $\pm 1 - 17\%$ uncertainty. The near eightfold increase only occurs at $\pm 1\%$ uncertainty, and stays below two beyond $\pm 5\%$ uncertainty.

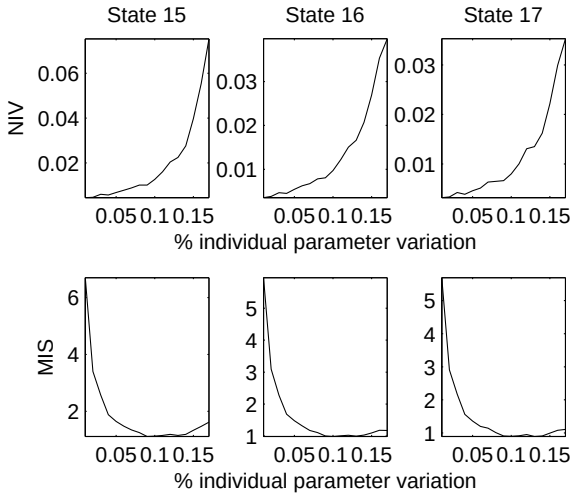

Figure 8. Multi-dimensional integral sensitivity (MIS) of starboard power supply currents for $\pm 1 - 17\%$ uncertainty.

3.3. Pulse Power System

We analyze uncertainty in a Simulink model (from the University of Texas at Austin) describing the operation of a large pulse load reflecting the power consumption of a rail gun [5]. The alternator is charged by accelerating its rotor to 18,000 rpm, at which point the inverter and charging motor are disconnected from the alternator and a shot is fired.

A six dimensional dimension-adaptive simulation using Clenshaw-Curtis quadrature was run, with $\pm 10\%$ uniform uncertainty in the alternator field winding resistance, primary generator one field winding leakage inductance, inductance of charging motor switches, and charging motor phase resistance, and $\pm 5\%$ uniform uncertainty in the 'on' configuration output rectifier diode resistance and charging motor excitation flux.

Fig. 9 shows mean trajectories with standard deviations for a few states, and 10 shows histograms at $t = 30$ seconds. A total of 53 system evaluations were required to attain an error tolerance of 10^{-3} for the charging motor phase one stator current. In most dimensions, the algorithm expended little effort, the highest order joint grid evaluated being level four in the dimension corresponding to the charging motor excitation flux and level three in that corresponding to the diode resistance, indicating some coupling between those parameters. A level three full grid would have used 729 points, taking much more time to achieve a comparable level of accuracy.

It can be seen from Fig. 9 that the primary generator phase voltage and the generator field winding voltage are sensitive to the simulated uncertainty, the first during charging before

the shot is fired and the latter afterward. The distributions at 30 seconds appear to mostly be Gaussian, with the exception of the generator speed, which is nearly uniform.

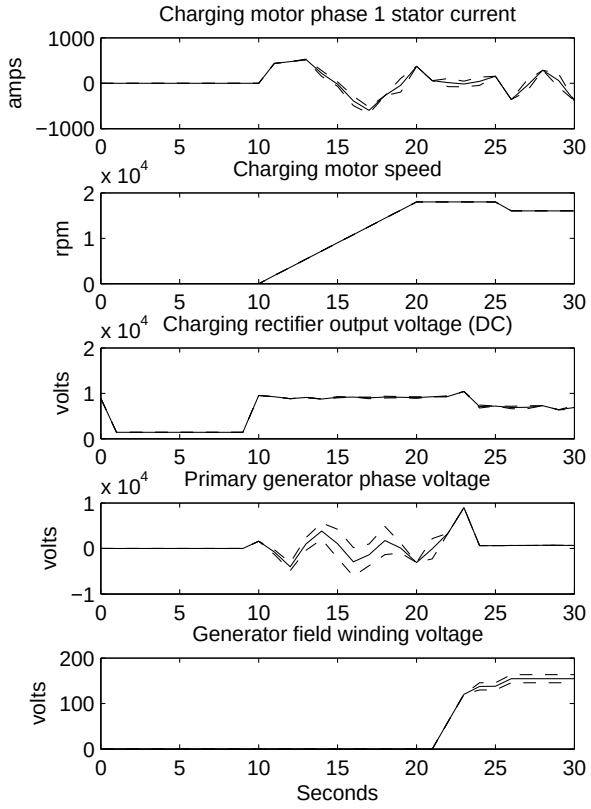

Figure 9. Mean trajectories with variance envelopes of rail gun states.

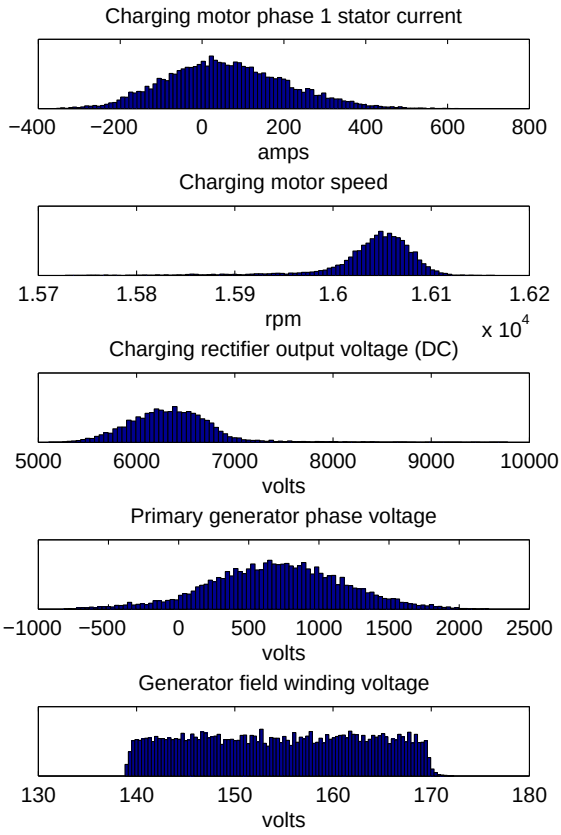

Figure 10. Histogram of rail gun states at $t = 30$ seconds.

4. CONCLUSION

We have presented collocation algorithms for efficiently solving stochastic differential equations with medium dimensional random spaces, and detailed how they can be applied to the uncertainty analysis of large-scale engineered systems, namely by computing statistical moments and PDF's from the solutions. Applications were given on a double pendulum, an integrated power system, and a pulse power system.

ACKNOWLEDGMENT

The work is supported by the Office of Naval Research, Grant N00014-02-1-0623 monitored by Dr. Terry Ericksen.

REFERENCES

[1] J. Berrut and L. Trefethen. Barycentric Lagrange interpolation. *SIAM Review*, 46(3):501–517, 2004.

[2] C. W. Clenshaw and A. R. Curtis. A method for numerical integration on an automatic computer. *Numerische Mathematik*, (2):197–205, 1960.

[3] P. J. Davis and P. Rabinowitz. *Methods of Numerical Integration*. Academic Press, New York, 1975.

[4] Philip J. Davis. *Interpolation and approximation*. Dover, New York, 1975.

[5] L. N. Domaschk, A. Ouroua, R. E. Hebner, O. E. Bowlin, and W. B. Colson. Coordination of large pulsed loads on future electric ships. *Magnetics, IEEE Transactions on*, 43(1):450–455, Jan. 2007.

[6] Zivi E. and McCoy T.J. Control of a shipboard integrated power system. In *Proceedings of the 33th An-*

nual Conference on Information Sciences and Systems, March 1999.

[7] S. Elhay and J. Kautsky. Generalized Kronrod-Patterson type imbedded quadratures. *Aplikace Matematiky*, 37(2):81–103, 1992.

[8] A. Genz. A package for testing multiple integration subroutines. In *Numerical Integration*, pages 337–340. Kluwer Academic Publishers, 1987.

[9] T. Gerstner and M. Griebel. Numerical integration using sparse grids. *Numerical Algorithms*, 18:209–232, 1998.

[10] T. Gerstner and M. Griebel. Dimension-adaptive tensor-product quadrature. *Computing*, 71(1):65–87, August 2003.

[11] Roger G. Ghanem and Pol D. Spanos. *Stochastic finite elements: a spectral approach*. Springer-Verlag New York, Inc., New York, NY, USA, 1991.

[12] Gene H. Golub and John H. Welsch. Calculation of gauss quadrature rules. Technical report, Stanford, CA, USA, 1967.

[13] George Em Karniadakis and Spencer J. Sherwin. *Spectral/hp Element Methods for CFD*. Oxford University Press, New York, 1999.

[14] Andreas Klimke. *Uncertainty modeling using fuzzy arithmetic and sparse grids*. PhD thesis, Universität Stuttgart, Shaker Verlag, Aachen, 2006.

[15] Peter E. Kloeden and Eckhard Platen. *Numerical Solution of Stochastic Differential Equations (Stochastic Modelling and Applied Probability)*. Springer, November 2000.

[16] PC Krause and Associates. Power system control development, final report, contract f33615-99-d-2974 for nsf/onr partnership in electric power network efficiency and security (epnes)). Technical report, March 2003.

[17] Harald Niederreiter. *Random number generation and quasi-Monte Carlo methods*. Society for Industrial and Applied Mathematics, Philadelphia, PA, USA, 1992.

[18] Bernt Oksendal. *Stochastic differential equations (3rd ed.): an introduction with applications*. Springer-Verlag New York, Inc., New York, NY, USA, 1992.

[19] T. N. L. Patterson. The optimum addition of points to quadrature formulae. *Mathematics of Computation*, 22(3):847–856, 1968.

[20] Krause P.C., Wasynczuk O., and Sudhoff S.D. *Analysis of Electric Machinery and Drive Systems*. IEEE Press and Wiley-Interscience, NY, second edition, 2002.

[21] W. H. Press, S. A. Teukolsky, W. T. Vetterling, and B. P. Flannery. *Numerical Recipes in C*. Cambridge University Press, second edition, 1992.

[22] Jean-Jacques E. Slotine and Haruhiko Asada. *Robot Analysis and Control*. John Wiley & Sons, Inc., New York, NY, USA, 1992.

[23] S. A. Smolyak. Quadrature and interpolation formulas for tensor products of certain classes of functions. *Dokl. Akad. Nauk SSSR*, 148:1042–1043, 1963. Russian, Engl. Transl.: Soviet Math. Dokl. 4:240–243, 1963.

[24] L. N. Trefethen. Is Gauss quadrature better than Clenshaw-Curtis? *SIAM Review*, 2007.

[25] Xiaoliang Wan and George Em Karniadakis. An adaptive multi-element generalized polynomial chaos method for stochastic differential equations. *J. Comput. Phys.*, 209(2):617–642, 2005.

[26] Dongbin Xiu and Jan S. Hesthaven. High-order collocation methods for differential equations with random inputs. *SIAM J. Sci. Comput.*, 27(3):1118–1139, 2005.

Biography

Josh A. Taylor received B.S. and M.S. degrees from Carnegie Mellon University and the Massachusetts Institute of Technology, respectively. He is currently working toward his Ph.D. degree in Mechanical Engineering.

Franz S. Hover is an Assistant Professor of Mechanical Engineering at the Massachusetts Institute of Technology. He received degrees from the Woods Hole Oceanographic Institution and MIT in oceanographic and mechanical engineering, held a post-doctoral fellowship at the Monterey Bay Aquarium Research Institute, and has consulted widely for industry. Research interests include applied dynamics and control, ocean vehicles and structures, and large-scale system design.

Abdelhamid Ouroua Abdelhamid Ouroua holds BS, MS, and PhD degrees in physics from the University of sciences and technology of Algiers, UCLA, and the University of Texas at Austin, respectively. His present work concentration is on electromagnetic design and analysis of electric machines.